

GameUIAgent: An LLM-Powered Framework for Automated Game UI Design with Structured Intermediate Representation

Wei Zeng, Fengwei An, Zhen Liu, and Jian Zhao

Abstract—Game UI design requires consistent visual assets across rarity tiers yet remains a predominantly manual process. We present GameUIAgent, an LLM-powered agentic framework that translates natural language descriptions into editable Figma designs via a *Design Spec JSON* intermediate representation. A six-stage neuro-symbolic pipeline combines LLM generation, deterministic post-processing, and a Vision-Language Model (VLM)-guided *Reflection Controller* (RC) for iterative self-correction with guaranteed non-regressive quality. Evaluated across 110 test cases, three LLMs, and three UI templates, cross-model analysis establishes a game-domain failure taxonomy (*rarity-dependent degradation*; *visual emptiness*) and uncovers two key empirical findings. A Quality Ceiling Effect (Pearson $r = -0.96$, $p < 0.01$) suggests that RC improvement is bounded by headroom below a quality threshold—a visual-domain counterpart to test-time compute scaling laws. A Rendering-Evaluation Fidelity Principle reveals that partial rendering enhancements paradoxically degrade VLM evaluation by amplifying structural defects. Together, these results establish foundational principles for LLM-driven visual generation agents in game production.

Index Terms—game user interface design, large language models, agentic iterative refinement, structured intermediate representation, VLM-as-judge

I. INTRODUCTION

Game user interface (UI) design fundamentally shapes player experience [1], [2]. Visual assets such as character cards and inventory thumbnails must balance aesthetic appeal, functional clarity, and thematic coherence—often across hundreds of elements spanning hierarchical rarity tiers (e.g., N/R/SR/SSR/UR in gacha-style games where collectible rarity governs visual fidelity). This remains a predominantly manual, labor-intensive process that constitutes a significant bottleneck in game art production pipelines [3].

Existing generative AI solutions typically target web interfaces or produce static raster images lacking editability. Figma-integrated approaches—Figma Make [4], GUIDE [5], and CoGen [6]—operate single-shot without quality verification and lack game-domain rules such as rarity hierarchies. We propose **GameUIAgent**, a neuro-symbolic pipeline that decouples LLM creative generation from deterministic rendering via a *Design Spec JSON* intermediate representation, closing the perception-action loop through an independent Vision-Language Model (VLM)-guided *Reflection Controller* (RC).

This work is supported by the Zhongguancun Academy (Grant No. C20250508). (Corresponding author: Jian Zhao.)

W. Zeng and F. An are with the School of Microelectronics, Southern University of Science and Technology (SUSTech), Shenzhen, China.

Z. Liu is with the School of Marxism, Tsinghua University, Beijing, China. W. Zeng, X. Li, Z. Liu, and J. Zhao are with the Zhongguancun Academy, Beijing, China (e-mail: jianzhao@zgci.ac.cn).

An experimental finding motivates a key design constraint: adding gradient rendering *without* correcting layout intent *worsens* VLM evaluation, because enhanced rendering exposes structural defects previously concealed by flat colors. We term this the **Rendering-Evaluation Fidelity Principle**. This paper makes three primary contributions:

- 1) **GameUIAgent and Design Spec JSON**: an end-to-end pipeline from natural language to editable Figma game UI designs with guaranteed non-regressive quality improvement.
- 2) A **game-domain failure taxonomy** for LLM-based structured UI generation: two task-structural failure modes—*rarity-dependent degradation* (complexity-overload in Gemini; inverse over-generation in GPT-4o-mini across the N/R/SR/SSR/UR hierarchy) and *visual emptiness* (syntactically valid JSON yielding blank renders)—establish that JSON validity is necessary but insufficient for design quality. Five objective structural metrics further reveal a *perceptual blind spot*: few-shot scaffolding governs compositional richness (+38% Node Count, +42% Color Diversity) invisible to VLM perceptual evaluation yet critical for production-grade output.
- 3) **Two empirical findings**: the **Quality Ceiling Effect** bounding iterative self-correction (Pearson $r = -0.96$ with initial quality), and the **Rendering-Evaluation Fidelity Principle** demonstrating how mismatched rendering fidelity can invert VLM reward signals—establishing foundational design principles for LLM-driven visual generation agents.

II. RELATED WORK

AI in Game UI Design. Recent surveys [7] identify UI asset creation as a key emerging LLM application in games. *pix2code* [8] and *Design2Code* [9] pioneered UI-to-code generation for web interfaces, while *LayoutGPT* [10] demonstrates compositional layout planning. These methods target standard interfaces ill-suited to the non-standard layouts of game UI. Two concurrent works address structured game UI directly: *AutoGameUI* [11] assembles UIs from existing designs via multimodal matching; *SpecifyUI* [12] extracts hierarchical IR from reference screenshots using designer feedback. Both differ fundamentally from GameUIAgent, which performs text-to-new-design generation combined with automated quality verification.

LLMs for Iterative Refinement and Evaluation. *Re-ACT* [13], *Reflexion* [14], and *SELF-REFINE* [15] demonstrate LLM improvement via verbal feedback. A critical limitation

remains: LLMs cannot reliably self-correct when acting as their own judges [16], [17], and self-improvement can degrade performance [18]. GameUIAgent mitigates this failure mode by sourcing feedback from an *independent* VLM critic and employing state-tracking to guarantee non-regressive improvement. The LLM-as-Judge paradigm [19] underpins our evaluator; to our knowledge, we provide the first Intra-class Correlation Coefficient [ICC(2,1)] [20], [21] reliability quantification for VLM-as-Judge on visual design quality.

Test-Time Compute Scaling. Recent work demonstrates that extending inference compute via iterative refinement can outperform scaling model parameters in certain regimes [22]. A critical open question is *when* additional refinement cycles yield diminishing returns. Our Quality Ceiling Effect provides a principled answer in the visual design domain: gain is bounded by evaluator headroom, not generator capacity, once output quality approaches the evaluator’s distinguishability threshold—making evaluator quality the primary lever for scaling agentic iterative refinement.

III. SYSTEM DESIGN

A. Overview

Fig. 1 illustrates GameUIAgent’s six-stage pipeline bridging natural language intent with professional design tools. Consistent with established agent frameworks [23], [24], the architecture integrates LLM-based creative generation, deterministic post-processing, and a self-correcting VLM-driven Reflection Controller. Concretely, the six stages are: (1) prompt engineering, (2) LLM generation of Design Spec JSON, (3) intelligent post-processing (repair, data injection, rarity enhancement), (4) renderer-based rasterization (Figma plugin or Python preview), (5) VLM quality review, and (6) Reflection Controller agentic loop. Three templates are supported: *Character Card* (320×450 px, vertical hierarchy), *Item Thumbnail* (96×96 px, compact grid), and *Skill Panel* (280×360 px, list composition). All prompts are centralized in a unified module; the system is model-agnostic, supporting any OpenAI-compatible LLM. A Python backend exposes HTTP REST endpoints that the Figma plugin queries to obtain finalized Design Spec JSON; a lightweight Python preview renderer enables high-throughput VLM evaluation without interactive Figma sessions.

B. Design Spec JSON

The *Design Spec JSON* schema is the central enabling contribution. It is *LLM-friendly* (natural naming aligned with pre-training data distributions), *tool-agnostic* (grounded in universal vector-graphics primitives transferable to Sketch or Adobe XD), and *expressive* (encoding gradient fills, drop shadows, and auto-layout constraints). The schema defines a recursive node tree in which each node specifies geometry (`x,y,width,height`), visual style (`fills, strokes, effects`), text content (`characters`), and hierarchical relationships (`children`). Four node types are supported: FRAME, RECTANGLE, ELLIPSE, and TEXT. A token budget of 6,000 per call accommodates complex UR-tier designs (average 4,534 tokens for DeepSeek V3).

C. Intelligent Post-Processing

Raw LLM outputs are enhanced in three deterministic phases. (1) **Repair**: color values are normalized (0–255 integer RGB to 0–1 float) and geometric dimensions clamped to positive integers. (2) **Data Injection**: stat bar widths are computed algorithmically from attribute values, achieving numerical precision beyond standard LLM capabilities. (3) **Rarity Enhancement**: a *Rarity Progression System* injects tier-scaled visual decorators across N/R/SR/SSR/UR—including star badges (0–5 icons), progressively upgraded border styles (simple strokes at N through multi-layer glow at UR), and element-specific thematic gradients.

D. VLM-Based Quality Review

A VLM evaluates generated designs across five dimensions: *Layout* (S_L , alignment and spacing), *Consistency* (S_C , color themes and font hierarchy), *Readability* (S_R , text contrast), *Completeness* (S_P , presence of required game elements), and *Aesthetics* (S_A , visual appeal and rarity appropriateness). Each dimension is scored 1–10 under a standardized rubric applied uniformly across all evaluation contexts.

E. Reflection Controller

The Reflection Controller (Algorithm 1) implements a self-correcting agentic loop inspired by SELF-REFINE [15] and Reflexion [14]. Given VLM scores $\mathbf{s} = (S_L, S_C, S_R, S_P, S_A)$, the controller identifies the two lowest-scoring dimensions and formulates a targeted Refinement Prompt with dimension-specific repair instructions (e.g., “Increase text contrast ratio > 4.5:1” for low S_R ; “Add missing `rarity_stars` nodes” for low S_P). This *surgical* repair strategy preserves correct elements while correcting only flagged deficiencies. The loop terminates when $S_{\text{avg}} \geq \theta$ (convergence) or $k = K$ (budget exhaustion), performing up to $K+1$ VLM evaluations in total ($k = 0, 1, \dots, K$); best-result tracking guarantees the returned Design Spec is never inferior to initial output. The sampling temperature is reduced from 0.7 to 0.5 during refinement to encourage conservative corrections.

The controller constitutes a finite-horizon Markov Decision Process (MDP) where defining the episode return as $G = \max_{0 \leq t \leq K} S_{\text{avg}}(\hat{q}_t)$ ensures best-result tracking yields non-regressive quality, precluding the score regression common in self-refining agents.

IV. EXPERIMENTS

Our experiments address four research questions. **RQ1 (Failure Taxonomy)**: what failure modes and reliability dimensions govern LLM-based structured game UI generation across models with different optimization targets. **RQ2 (Component Contribution)**: impact of individual prompt components and post-processing. **RQ3 (Generalization)**: adaptability across UI templates and renderer configurations. **RQ4 (Agentic Refinement)**: RC effectiveness and the Quality Ceiling Effect. Code and data available at <https://github.com/zengwei-code/GameUIAgent>.

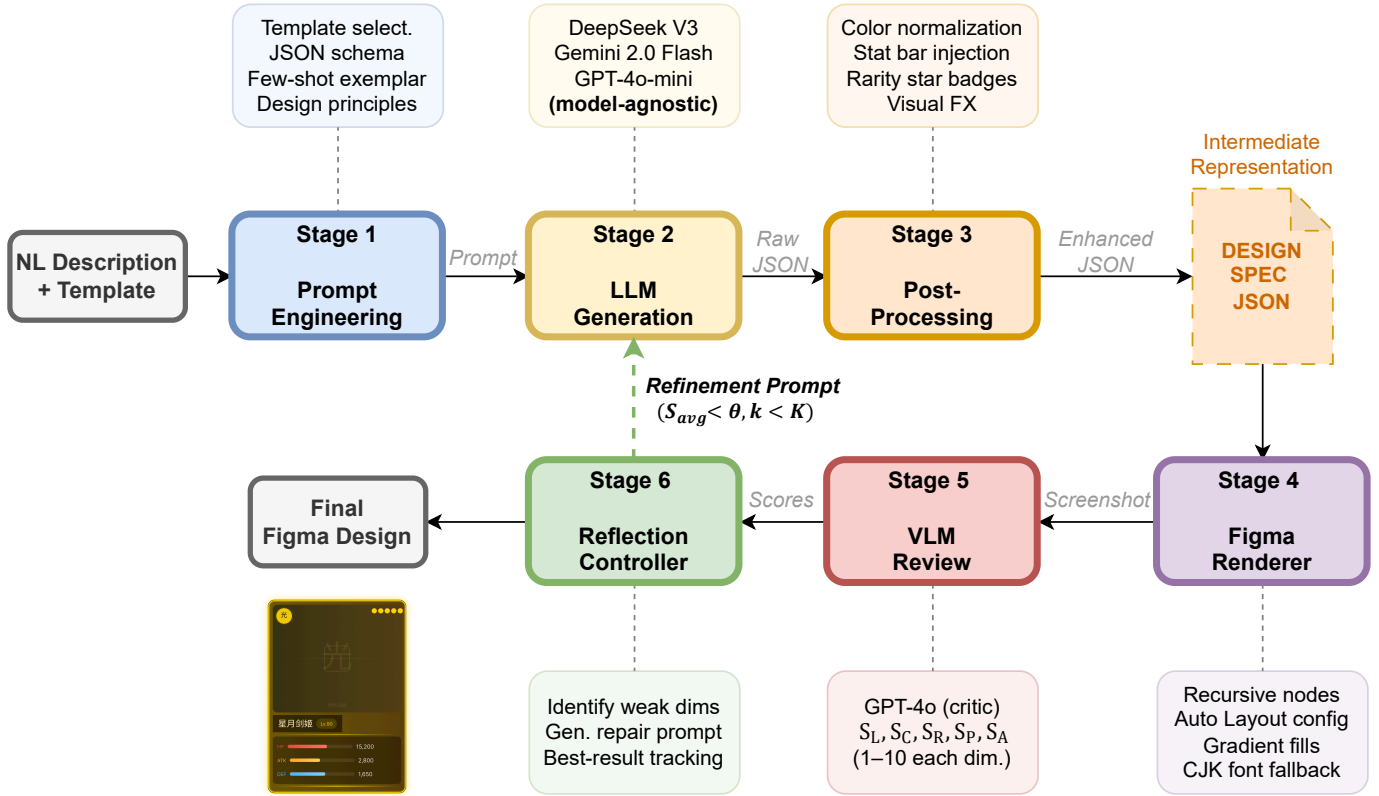


Fig. 1. Overall architecture of GameUIAgent. Stages 1–5 constitute the forward generation pass; Stage 6 (Reflection Controller, green) closes the agentic loop by converting VLM quality scores into targeted repair prompts and re-invoking Stage 2 if $S_{avg} < \theta$. The *Design Spec JSON* intermediate representation (dashed box) separates creative generation from deterministic enhancement.

Algorithm 1 Reflection Controller with Best-Result Tracking

Input: $spec_0, \theta$ (threshold), K (max iter)
Output: $spec^*$ (best Design Spec)
 $spec^* \leftarrow spec_0, s^* \leftarrow 0, k \leftarrow 0$
while $k \leq K$ **do**
 $I_k \leftarrow \text{RENDER}(spec_k)$
 $s_k \leftarrow \text{VLMREVIEW}(I_k, \text{rubric})$
 if $s_{avg,k} > s^*$ **then**
 $spec^* \leftarrow spec_k, s^* \leftarrow s_{avg,k}$
 end if
 if $s_{avg,k} \geq \theta$ **or** $k = K$ **then**
 break
 end if
 $\mathcal{W} \leftarrow \text{BOT2}(s_k)$ {Two lowest dims}
 $p_{refine} \leftarrow \text{GENREPAIRPROMPT}(\mathcal{W}, s_k)$
 $spec_{k+1} \leftarrow \text{LLMREFINE}(spec_k, p_{refine}, T=0.5)$
 $k \leftarrow k + 1$
end while
return $spec^*$

Fig. 2 presents a qualitative overview of GameUIAgent’s outputs across all five rarity tiers (DeepSeek V3, Fire element theme), illustrating the progressive visual enrichment injected automatically by the post-processing pipeline. Quantitative

evaluation of these outputs follows in the sections below.

A. Experimental Setup

Models. The framework accepts any OpenAI-compatible API endpoint, enabling straightforward replication with current-generation models. Three representative LLMs spanning distinct optimization targets are evaluated via OpenRouter to characterize failure modes across the quality–cost–speed design space: **DeepSeek V3** [25] (MoE, 671B params, quality-optimized, \$0.008/call) serves as the primary generator; **Gemini 2.0 Flash** [26] represents speed- and cost-optimized inference (\$0.001/call); **GPT-4o-mini** [27] represents general-purpose instruction-following at moderate scale (\$0.012/call). **GPT-4o** [28] serves as the automated VLM critic.

Templates and Test Cases. 110 cases total: *Character Card* (50 cases: 5 rarity tiers \times 10 characters per tier, spanning 5 element types: Fire, Water, Wind, Light, Dark), *Item Thumbnail* (30 cases, 96×96 px), and *Skill Panel* (30 cases, list-based composition).

Metrics. JSON Validity Rate (V), VLM Quality Scores (S , 1–10 per dimension), latency (T), and token count. Three progressively capable renderer configurations enable controlled comparisons: *Flat* (solid colors only), *Gradient* (adds linear fills and drop shadows), and *Layout-aware* (adds Auto Layout simulation resolving child coordinate conflicts prior to rasterization). Five structural metrics—Node Count (NC), Canvas



Fig. 2. Rarity progression (N to UR) generated by GameUIAgent with DeepSeek V3. Progressively richer visual treatments are injected automatically: simple gray borders (N) → colored theme borders (R) → gradient fills with glow (SR) → multi-layered borders with star badges (SSR) → golden ornate frames (UR). All five cards share the Fire element theme, demonstrating consistent thematic adaptation across the rarity hierarchy.

Coverage (COV), Color Diversity (CD), Text Contrast Ratio (CR), Element Completeness (EC)—are computed directly from Design Spec JSON without rendering.

Evaluator Reliability. Three independent GPT-4o runs on 49 DeepSeek V3 designs yield within-VLM ICC(2,1) = 0.555 [20], [21] (fair, per Cicchetti’s guidelines), with stable aggregate means (8.02, 8.03, 8.06; mean per-design MAD = 0.15). Since the RC compares successive iterations of the *same* design under the *same* evaluator, within-VLM reliability is the operative metric validating single-evaluator RC design. A supplementary multi-VLM panel (GPT-4o [28], Claude-3.5-Sonnet [29], Gemini 2.0 Flash [26]; $n = 20$ stratified designs) reveals **VLM Quality Perception Divergence**: cross-VLM ICC(2,1) = 0.021, $K\alpha = -0.088$ [30], driven by scale saturation (GPT-4o $\sigma = 0.40$ vs. Gemini $\sigma = 0.28$) and substantive disagreement on Completeness (GPT-4o: 5.65 vs. Claude: 7.15, reflecting differing views on Figma-native vs. schema-level coverage). Aesthetics is the sole dimension with positive cross-VLM agreement ($\alpha = 0.023$), confirming holistic visual appeal as the most model-invariant dimension.

B. RQ1: LLM Failure Taxonomy and Cross-Model Analysis

Table I reveals that *structural reliability* (JSON validity) and *per-output perceptual quality* are orthogonal performance dimensions in structured UI generation: Gemini 2.0 Flash (88%, 6.4/10) and GPT-4o-mini (56%, 6.7/10) achieve near-equivalent VLM scores despite a 32-point validity gap, confirming that schema conformance reliability—not single-output perceptual quality—is the primary cross-model differentiator. All pairwise quality differences are statistically significant (Mann-Whitney $p < 0.001$). DeepSeek V3 leads on both dimensions (98.0% validity, 8.0/10, $S_C = 8.9$), establishing it as the primary generator for RQ2–RQ4. As noted in Table I, DeepSeek V3 scores reflect Figma renders while others use preview renders; the renderer comparison (§IV-D) bounds this confound at ≤ 1.58 points, so the quality gaps partially reflect renderer fidelity differences.

Two **task-structural failure modes** characterize LLM-based structured UI generation independent of specific model capability levels. **Rarity-dependent degradation** manifests with divergent signatures: Gemini’s validity degrades monotonically from 100% (N-tier) to 60% (UR-tier), exposing a *complexity-overload* pattern; GPT-4o-mini shows an inverse trend (30% at N), revealing an *over-generation* pattern on structurally simple inputs. These divergent signatures reflect each model’s distinct structural capacity ceiling rather than general competence. **Visual emptiness**—syntactically valid JSON rendering as blank frames due to zero-area child nodes or indistinguishable background colors—further establishes that $V = 100\%$ is necessary but insufficient for design quality, motivating the multi-dimensional evaluation framework of §IV-A. Objective structural analysis reinforces these findings: GPT-4o-mini generates the highest node density (NC = 26.0 ± 1.6) and element completeness (EC = 0.99) yet achieves the lowest perceptual scores ($S_{\text{avg}} = 6.7$), confirming that visual harmony outweighs raw element density. Among all structural metrics, Text Contrast Ratio is the strongest single predictor of VLM quality for DeepSeek V3 ($r = 0.51$, $p < 0.001$, $n = 49$), reflecting the central role of legibility in game UI appeal. Fig. 3 illustrates representative failure cases and a cross-model visual comparison.

C. RQ2: Ablation and Baseline Study

Table II reports ablation results on 50 Character Card cases (DeepSeek V3). Three findings stand out.

Structured prompt design is essential. The No-Schema baseline achieves 100% validity yet VLM quality collapses to 4.8/10 ($\Delta = -3.1$ vs. No Few-Shot on matched renderers, $p < 0.001$), establishing that the schema, domain rules, and color system—not raw model capability—are the primary quality enablers. Structural metrics corroborate: Canvas Coverage plummets from 1.96 to 0.05 and Color Diversity falls 61%.

Post-processing is the critical perceptual driver. Disabling it reduces overall quality by 1.4 points ($p < 0.001$,

TABLE I

CROSS-MODEL COMPARISON ON CHARACTER CARD GENERATION ($n=50$). *Note:* DEEPSEEK V3 SCORES ARE FROM FIGMA RENDERS; OTHER MODELS USE PREVIEW RENDERS. THE RQ3 RENDERER COMPARISON (TABLE III) ESTIMATES A FIGMA ADVANTAGE OF UP TO +1.58 POINTS, IMPLYING THAT CROSS-MODEL QUALITY GAPS REFLECT BOTH MODEL CAPABILITY AND RENDERER DIFFERENCES.

Model	$V(\%)$	$T(s)$	Tokens	S_L	S_C	S_R	S_P	S_A	S_{avg}	\$/call
DeepSeek V3 [†]	98.0	47.0	4,534	8.1±0.4	8.9±0.4	7.9±0.5	7.1±0.6	8.1±0.5	8.0±0.3	0.008
Gemini 2.0 Flash [‡]	88.0	14.7	5,141	6.6±0.6	7.2±0.8	5.6±0.7	6.1±0.9	6.4±0.6	6.4±0.6	0.001
GPT-4o-mini [‡]	56.0	35.2	4,485	6.9±0.4	7.3±0.8	6.0±0.5	6.5±0.8	6.6±0.5	6.7±0.4	0.012

[†] VLM on Figma renders ($n=49$). [‡] VLM on preview renders (Gemini $n=44$, GPT-4o-mini $n=28$).

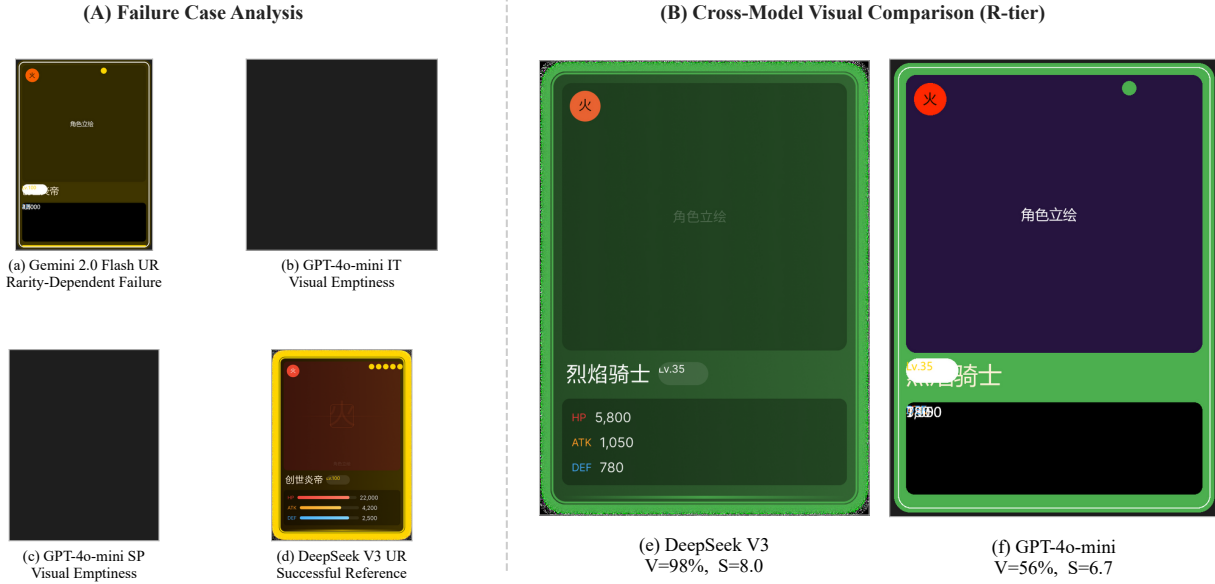


Fig. 3. Cross-model analysis. (A) Failure cases (left panel): (a) Gemini UR-tier degradation ($V = 60\%$); (b–c) GPT-4o-mini visual emptiness on Item Thumbnail and Skill Panel; (d) DeepSeek V3 UR reference. (B) R-tier comparison (right panel, enlarged for clarity): DeepSeek V3 (left, $S = 8.0$) produces coherent themed borders, readable color-coded stats, and a well-structured portrait region; GPT-4o-mini (right, $S = 6.7$) yields a syntactically valid design but with low-contrast text, blank portrait region, and element overlap.

paired Wilcoxon), with the largest gain in Readability (+2.2), driven by color normalization correcting text-background contrast deficiencies. Structurally, however, post-processing leaves the design tree intact: Full Pipeline and No Post-Process share near-identical structural profiles ($NC = 23.4$, $EC = 0.93$), confirming it refines within-node graphical fidelity without altering tree topology—a sub-structural operation with disproportionate perceptual impact.

Few-shot acts as a structural amplifier. Removing the exemplar reduces Node Count by 38%, Canvas Coverage by 39%, and Color Diversity by 42% while exerting negligible impact on VLM perceptual scores ($\Delta = -0.1$)—demonstrating that the exemplar governs compositional richness that lies in a *perceptual blind spot* invisible to VLM evaluation. Counterintuitively, latency increases ($47\text{ s} \rightarrow 79\text{ s}$) despite fewer output tokens ($4,534 \rightarrow 3,557$), attributable to increased server-side generation time without a structural scaffold.

D. RQ3: Template Generalization and Rendering Fidelity

The pipeline generalizes across all three templates without modification. Token consumption scales with structural

TABLE II
ABLATION AND BASELINE STUDY (DEEPSEEK V3, $n=50$)

Config.	$V(\%)$	$T(s)$	Tok.	S_{avg}	S_L	S_R	S_A
Full Pipeline [†]	98.0	47	4,534	8.0	8.1	7.9	8.1
No Few-Shot [‡]	96.0	79	3,557	7.9	8.0	7.9	7.5
No Post-Proc. [‡]	96.0	47	4,534	6.5	6.7	5.7	6.5
No-Schema [‡]	100.0	20	728	4.8	4.9	4.7	4.8

Δ^{\ddagger} | — — — | +3.1 +3.1 +3.2 +2.7
[†]Figma renders. [‡]Preview renders. Δ^{\ddagger} : No-FS minus No-Schema (matched renders).

complexity (Item Thumbnail: 1,008; Character Card: 4,534; Skill Panel: 6,165 tokens). Item Thumbnail achieves 100% validity at 24.8 s; Skill Panel shows 90% validity at 88.7 s with failures clustering at R/SSR/UR tiers, consistent with the rarity-complexity effect in RQ1.

A controlled renderer comparison ($n=27$ Skill Panels, identical Design Spec JSONs) reveals the **Rendering-Evaluation Fidelity Principle**: adding gradients/shadows *without* layout correction *degrades* VLM scores from 4.42 to 3.44 ($p = 0.0017$, $d = -0.81$). The Layout-aware renderer—which re-

TABLE III
CONTROLLED RENDERER COMPARISON: SAME 27 SKILL PANEL DESIGNS
EVALUATED ACROSS THREE CONFIGURATIONS (PAIRED WILCOXON
SIGNED-RANK)

Renderer	S_{avg}	S_R	S_C	Δ vs. prev	p	d
Flat (solid colors only)	4.42±1.01	4.46	5.38	—	—	—
Gradient (+grad./shadows, no layout)	3.44±0.63	2.74	4.44	-1.00 ^a	0.0017	-0.81
Layout-aware (+Auto Layout simulation)	5.96±0.84	4.82	6.93	+2.52 ^b	<0.001	2.74
Net Flat→Layout-aware	—	—	—	+1.58 ^c	0.0001	1.16

^a Gradient amplifies overlap salience (S_R : -1.73, $p < 0.001$, $d = -1.38$).

^b Auto Layout simulation eliminates overlaps before rasterization.

^c Net S_R not significant (+0.38, $p = 0.18$); Tier-1 harm partially offsets recovery.

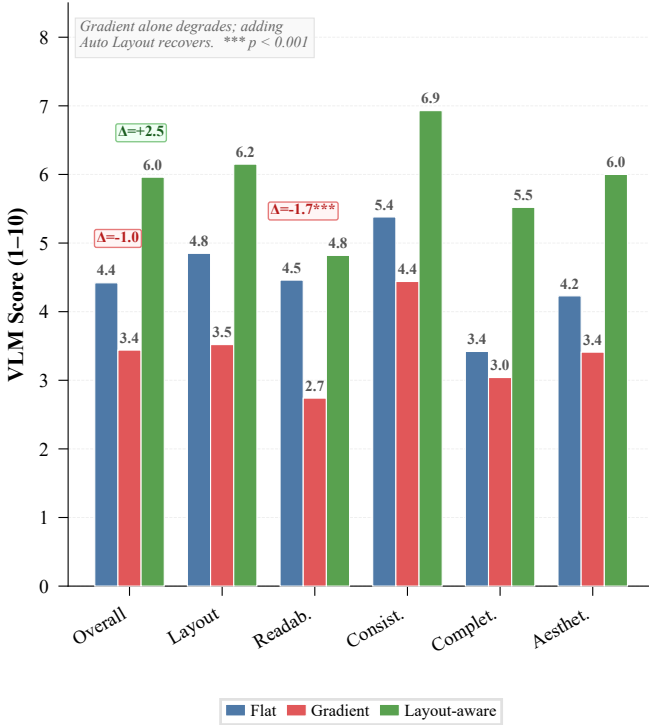


Fig. 4. Rendering-Evaluation Fidelity: the Gradient renderer *decreases* VLM score by -1.00 ($p = 0.0017$, $d = -0.81$) relative to the Flat baseline; the Layout-aware renderer recovers and surpasses it ($\Delta = +2.52$, $p < 0.001$, $d = 2.74$). $n = 27$ Skill Panel designs evaluated across three renderer configurations with identical Design Spec JSONs.

solves child coordinate conflicts via Auto Layout simulation *before* rasterization—recovers to 5.96 ($\Delta = +2.52$, $p < 0.001$, $d = 2.74$). Table III reports the full per-dimension breakdown. Gradient shading amplifies the visual salience of overlapping elements (Readability drop: -1.73 , $p < 0.001$, $d = -1.38$), converting latent layout defects into highly visible flaws that the VLM penalizes sharply. Fig. 4 visualizes this two-tier bottleneck.

E. RQ4: Agentic Refinement via Reflection Controller

Table IV reports RC results on 28 valid Character Card cases (DeepSeek V3, Gradient renderer, $K \leq 2$, $\theta = 7.5$). The Gradient renderer is used here rather than Layout-aware, so that RC gains are attributable to the iterative repair loop rather than renderer-side overlap resolution—thereby isolat-

TABLE IV
REFLECTION CONTROLLER RESULTS BY RARITY TIER (DEEPSEEK V3,
GRADIENT RENDERER, $K \leq 2$, $\theta = 7.5$; WILCOXON: $W = 0$, $p < 0.001$,
 $d = 1.30$).

Metric	N ($n=10$)	R ($n=9$)	SR ($n=9$)	All ($n=28$)
Init S_{avg}	5.30±0.48	5.56±0.78	7.00±0.50	5.93±0.98
Final S_{avg}	6.40±0.70	6.67±1.00	7.67±0.50	6.89±0.92
Avg Δ	+1.10	+1.11	+0.67	+0.96
Improved / Same	9/1	7/2	5/4	21/7
Regression-free	10/10	9/9	9/9	28/28 (100%)
Final ≥ 7.5	0/10	2/9	6/9	8/28 (28.6%)

Note: SSR/UR excluded (init $\geq \theta$); headroom at init=7.66 gives $\Delta = +0.07$ (Quality Ceiling Effect).

ing the RC’s intrinsic correction capacity. The RC achieves mean $\Delta = +0.96$ ($W = 0$, $p < 0.001$, $d = 1.30$, 95% CI [+0.68, +1.25]). Best-result tracking yields 100% regression-free outcomes (all 28 cases at or above initial score); only 7.7% experience a transient Iter-1 score dip. The best single-case gain is CC-020 (5.0 → 8.0, $\Delta = +3.0$). Gains are consistent across rarity tiers (N: +1.10, R: +1.11, SR: +0.67).

Quality Ceiling Effect. Compiling five independent RC conditions spanning DeepSeek V3 and GPT-4o-mini configurations, five tier mixes, and three iteration budgets ($n_{\text{total}} = 93$ valid cases), RC improvement exhibits a near-perfect negative correlation with mean initial quality: Pearson $r = -0.96$ ($p < 0.01$, $t = -5.9$, $df = 3$), spanning initial scores from 5.93 ($\Delta = +0.96$) to 7.66 ($\Delta = +0.07$). Given the five-condition aggregate ($df = 3$), this correlation is exploratory evidence for the headroom hypothesis rather than a precisely fitted universal law; replication with additional generator configurations is warranted. This documents *critique saturation*: as designs approach θ , VLM critiques shift to increasingly marginal issues, diminishing repair precision. Skip rates (initial score $\geq \theta$) scale monotonically with initial quality from 3.6% to 65.5%, and all 93 cases remain regression-free. The renderer comparison—Flat ($\Delta = 0.00$, dip rate 76%) → Gradient ($\Delta = +0.96$, dip rate 7.7%)—indicates evaluation fidelity as a primary limiting factor for RC effectiveness. Fig. 5 visualizes the Quality Ceiling Effect. Fig. 6 shows trajectories from a supplementary $K \leq 3$ ablation on the 10 N-tier cases (DeepSeek V3, Gradient renderer): CC-001 exhibits a plateau-breaking pattern (7.0 → 7.0 → 6.4 → 8.0) inaccessible at $K \leq 2$; best-result tracking prevents CC-006’s $K = 3$ regression.

V. DISCUSSION

Design Principles. The ablation establishes an actionable hierarchy for LLM-driven UI generation: *structured prompt design* is the foundational quality enabler; *post-processing* is the primary perceptual driver (+1.4 VLM, +2.2 Readability; Wilcoxon, No-FS vs. No-Post-Proc on matched preview renderers); and the *few-shot exemplar* functions as a structural amplifier (38% Node Count gain) whose contribution is invisible to VLM perceptual evaluation but critical for compositional richness. All three components are non-negotiable in production deployment.

Rendering-Evaluation Fidelity Principle. Formally, let $\hat{q}_t = \text{VLM}(\text{render}(d_t))$ denote the observable quality signal for design d_t with true quality q_t . Under the Gradient renderer,

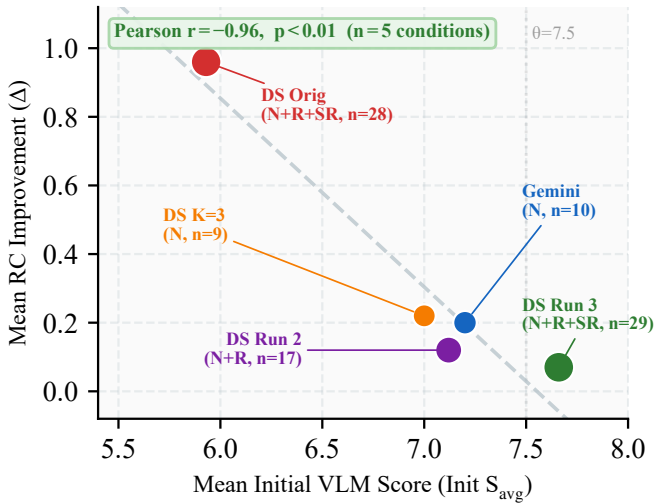


Fig. 5. Quality Ceiling Effect: Pearson $r = -0.96$ ($p < 0.01$) between mean initial VLM score and RC improvement (Δ) across five independent conditions ($n_{total} = 93$; DeepSeek V3 and GPT-4o-mini; five tier mixes). RC gain is universally bounded by headroom below θ , not by model capability or rarity complexity.

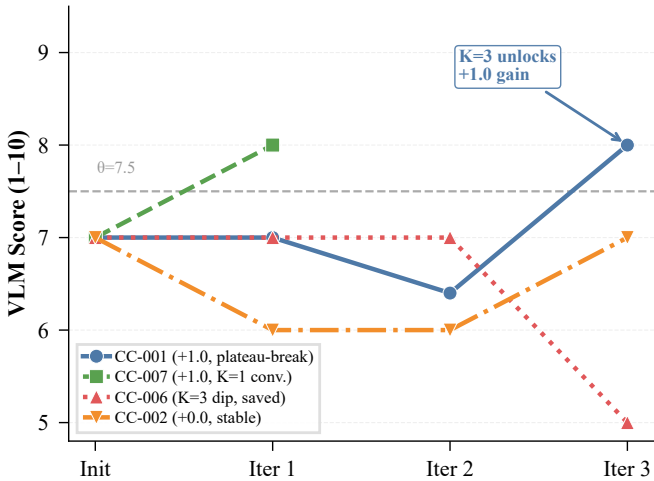


Fig. 6. $K \leq 3$ N-tier ablation: RC score trajectories for representative cases. CC-001 exhibits a plateau-breaking pattern ($7.0 \rightarrow 7.0 \rightarrow 6.4 \rightarrow 8.0$) inaccessible at $K \leq 2$; CC-007 converges at $K = 1$; best-result tracking prevents CC-006’s $K = 3$ regression. Dashed line: $\theta = 7.5$.

$\hat{q}_t < q_t$: gradient shading amplifies the salience of overlapping elements concealed by flat colors, inverting the VLM reward signal. Under the Layout-aware renderer, $\hat{q}_t \approx q_t$, since Auto Layout simulation resolves overlaps prior to graphical enhancement. Consequently, synchronized improvements across both rendering tiers—graphical fidelity and spatial correctness—are necessary for reliable agentic refinement. The Quality Ceiling Effect ($r = -0.96$) quantifies reward saturation in the visual domain, drawing a direct parallel to test-time compute scaling laws [22]. These principles apply broadly to any LLM agent that synthesizes structured visual specifications and refines them based on rendered perceptual

feedback.

Practical RC Deployment. The Quality Ceiling Effect translates directly into a tier-aware compute allocation policy: (i) if $init < 6.0$, apply $K \leq 2$ RC cycles (expected $\Delta > +0.9$); (ii) if $6.0 \leq init < 7.5$, $K \leq 2$ is recommended ($\Delta \approx +0.5-0.7$); (iii) if $init \geq 7.5$, RC should be skipped ($\Delta \approx 0$); and (iv) upon detecting a late-iteration score dip within $K \leq 2$ (e.g., $s_{k=2} < s^*$), extending to $K \leq 3$ may exploit a plateau-breaking event (as in CC-001, $7.0 \rightarrow 7.0 \rightarrow 6.4 \rightarrow 8.0$, inaccessible at $K \leq 2$). The threshold $\theta = 7.5$ performs consistently across the conditions evaluated here; practitioners should calibrate it to approximately the 80th percentile of their generator’s output distribution.

Limitations. The evaluation covers RPG gacha UIs exclusively; FPS HUDs and RTS minimaps remain unvalidated. The current schema supports four primitive node types, whereas production demands vector paths and image fills. Portrait regions are rendered as placeholders, and animation or interactive states are not modeled. Cross-template comparisons involve heterogeneous rendering environments; this confound is bounded at ≤ 0.1 points by restricting Δ comparisons to renderer-consistent conditions. The cross-model comparison (RQ1) reflects three representative API configurations spanning the quality–cost–speed design space; the identified failure modes—rarity-dependent degradation and visual emptiness—are posited as task-structural properties of LLM-based structured generation, expected to persist across model generations, while specific validity rates and quality scores will shift with newer generators. The framework’s model-agnostic design and released 110-case evaluation suite support direct replication with current SoTA models. Beyond model coverage, the primary limitation of the current work is the absence of human expert evaluation. All quality assessments rely on GPT-4o as an automated VLM critic; while $ICC(2,1) = 0.555$ confirms adequate within-evaluator reliability for comparative analyses, external validity—the correlation between VLM scores and professional designer judgment—remains unestablished. Recent work on LLM-as-Judge has demonstrated moderate-to-strong agreement with human annotators in adjacent domains [19], and our per-design stability (mean MAD = 0.15 across three evaluation runs) suggests systematic rather than random scoring. Nevertheless, a formal human expert study is a necessary next step for deployment validation.

VI. CONCLUSION

We present GameUIAgent, a neuro-symbolic framework bridging natural language descriptions and professional game UI design through a *Design Spec JSON* intermediate representation. By combining LLM generation with an independent VLM-driven Reflection Controller, the system delivers editable Figma outputs with a formal guarantee of non-regressive quality improvement across 110 evaluated cases.

A cross-model failure taxonomy establishes *rarity-dependent degradation* and *visual emptiness* as task-structural failure modes persistent across LLM families, with structural analysis revealing a *perceptual blind spot* where few-shot

scaffolding governs compositional richness (+38% NC, +42% CD) invisible to VLM perceptual scoring. Two empirical findings further establish foundational principles for visual agentic systems. The **Quality Ceiling Effect** ($r = -0.96$) reveals that iterative improvement is bounded by evaluator headroom—where *evaluation capability*, not generation power, becomes the limiting factor. The **Rendering-Evaluation Fidelity Principle** warns that incomplete rendering enhancements paradoxically invert reward signals by amplifying structural defects. As AI tools evolve from single-shot generation toward autonomous iterative refinement in game production, rigorous alignment among structural constraints, rendering fidelity, and evaluation mechanisms will be paramount. The framework’s model-agnostic design and released 110-case evaluation suite enable direct replication as more capable LLMs emerge, extending these findings beyond the three model configurations evaluated here.

REFERENCES

- [1] T. Fullerton, *Game Design Workshop: A Playcentric Approach to Creating Innovative Games*, 4th ed. Boca Raton, FL: CRC Press, 2018.
- [2] J. Schell, *The Art of Game Design: A Book of Lenses*, 3rd ed. Boca Raton, FL: CRC Press, 2019.
- [3] E. Adams, *Fundamentals of Game Design*, 3rd ed. Berkeley, CA: New Riders, 2014.
- [4] Figma Inc., “Introducing Figma Make: Prompt-driven interactive design,” Tech. Rep., 2025. [Online]. Available: <https://www.figma.com/blog/introducing-figma-make> [Accessed: Mar. 7, 2026].
- [5] K. Kolthoff, F. Kretzer, C. Bartelt, A. Maedche, and S. P. Ponzetto, “GUIDE: LLM-driven GUI generation decomposition for automated prototyping,” *arXiv preprint arXiv:2502.21068*, 2025.
- [6] I. Kanapathipillai and O. Priyankara, “CoGen: Creation of reusable UI components in Figma via textual commands,” *arXiv preprint arXiv:2601.10536*, 2026.
- [7] R. Gallotta *et al.*, “Large language models and games: A survey and roadmap,” *IEEE Trans. Games*, 2024, doi: 10.1109/TG.2024.3461510.
- [8] T. Beltramelli, “pix2code: Generating code from a graphical user interface screenshot,” in *Proc. ACM EICS*, 2018, Art. no. 3, 6 pages, doi: 10.1145/3220134.3220135.
- [9] C. Si, Y. Zhang, R. Li, Z. Yang, R. Liu, and D. Yang, “Design2Code: Benchmarking multimodal code generation for automated front-end engineering,” in *Proc. NAACL*, 2025, pp. 3956–3974.
- [10] W. Feng *et al.*, “LayoutGPT: Compositional visual planning and generation with large language models,” in *Proc. NeurIPS*, 2023.
- [11] Z. Tang, Q. Cheng, M. Tan, Y. Zhang, and F. Xia, “AutoGameUI: Constructing high-fidelity GameUI via multimodal correspondence matching,” *arXiv preprint arXiv:2411.03709*, 2024.
- [12] Y. Chen, C. Shi, and L. Chen, “SpecifyUI: Supporting iterative UI design intent expression through structured specifications and generative AI,” *arXiv preprint arXiv:2509.07334*, 2025.
- [13] S. Yao *et al.*, “ReAct: Synergizing reasoning and acting in language models,” in *Proc. ICLR*, 2023.
- [14] N. Shinn *et al.*, “Reflexion: Language agents with verbal reinforcement learning,” in *Proc. NeurIPS*, 2023.
- [15] A. Madaan *et al.*, “SELF-REFINE: Iterative refinement with self-feedback,” in *Proc. NeurIPS*, 2023.
- [16] J. Huang *et al.*, “Large language models cannot self-correct reasoning yet,” in *Proc. ICLR*, 2024.
- [17] R. Kamoi *et al.*, “When can LLMs actually correct their own mistakes? A critical survey of self-correction of LLMs,” *arXiv preprint arXiv:2406.01297*, 2024.
- [18] W. Zhao *et al.*, “Large language model agents are not always faithful self-evolvers,” *arXiv preprint arXiv:2601.22436*, 2026.
- [19] L. Zheng *et al.*, “Judging LLM-as-a-judge with MT-Bench and Chatbot Arena,” in *Proc. NeurIPS*, 2023.
- [20] P. E. ShROUT and J. L. Fleiss, “Intraclass correlations: Uses in assessing rater reliability,” *Psychological Bulletin*, vol. 86, no. 2, pp. 420–428, 1979.
- [21] D. V. Cicchetti, “Guidelines, criteria, and rules of thumb for evaluating normed and standardized assessment instruments in psychology,” *Psychological Assessment*, vol. 6, no. 4, pp. 284–290, 1994.
- [22] C. Snell, J. Lee, K. Xu, and A. Kumar, “Scaling LLM test-time compute optimally can be more effective than scaling model parameters,” in *Proc. ICLR*, 2025.
- [23] L. Wang *et al.*, “A survey on large language model based autonomous agents,” *Frontiers of Computer Science*, vol. 18, no. 6, p. 186345, 2024.
- [24] Anthropic, “A practical guide to building agents,” Tech. Rep., 2025. [Online]. Available: <https://www.anthropic.com/research/building-effective-agents> [Accessed: Mar. 7, 2026].
- [25] DeepSeek-AI, “DeepSeek-V3 technical report,” *arXiv preprint arXiv:2412.19437*, 2024.
- [26] Google DeepMind, “Gemini 2.0 Flash,” Tech. Rep., 2025. [Online]. Available: <https://deepmind.google/technologies/gemini/flash/> [Accessed: Mar. 7, 2026].
- [27] OpenAI, “GPT-4o mini: Advancing cost-efficient intelligence,” 2024. [Online]. Available: <https://openai.com/index/gpt-4o-mini-advancing-cost-efficient-intelligence/> [Accessed: Mar. 7, 2026].
- [28] OpenAI, “Hello GPT-4o,” 2024. [Online]. Available: <https://openai.com/index/hello-gpt-4o/> [Accessed: Mar. 7, 2026].
- [29] Anthropic, “Claude 3.5 Sonnet,” 2024. [Online]. Available: <https://www.anthropic.com/news/claude-3-5-sonnet> [Accessed: Mar. 7, 2026].
- [30] K. Krippendorff, *Content Analysis: An Introduction to Its Methodology*, 2nd ed. Thousand Oaks, CA: SAGE Publications, 2004.